Reduction of Root-Mean-Square Error in Faceted Space Antennas

W. B. Fichter*
NASA Langley Research Center, Hampton, Virginia

This paper examines the potential for reducing root-mean-square surface error in shallow faceted reflectors by replacing flat facets with laterally curved membrane facets. Exact solutions are obtained for the small lateral deflections of equilateral triangular and rectangular membranes subject to isotropic tension and parabolic edge deflections. These solutions are used to minimize the rms error between a facet of a shallow paraboloidal surface and its approximating membrane facet. The resulting optimum placements and edge curvatures yield membrane facets which have significantly lower rms errors than the corresponding best-fit flat facets. The rms error reductions are about 55% for equilateral triangles and 25-93% for rectangles, depending on aspect ratio. The results suggest that replacement of flat facets with membrane facets conforming to curved structural members could yield reflectors with lower rms-error, or comparable error with larger facets and, hence, fewer structural members.

Introduction

MANY of the large-aperture space antennas currently envisioned are shallow parabolic dishes with faceted reflecting surfaces. Substitution of an assemblage of flat facets for the ideal smooth paraboloidal surface necessarily introduces surface errors which degrade antenna performance. One means of reducing the root-mean-square error is to make the facets smaller. For example, Agrawal et al.[1] obtained expressions for the rms error incurred by replacing a shallow spherical dish by an assemblage of flat facets in the shape of equilateral triangles, squares, and regular hexagons. These expressions were used to obtain estimates of flat-facet size required to satisfy a prescribed tolerance limit on surface rms error. It was also shown therein that for shallow reflectors the ideal paraboloidal surface could be replaced with insignificant error by a spherical surface.

Meyer[2] used linear membrane theory to derive expressions for rms error in faceted, knitted-mesh reflectors of cylindrical parabolic or axisymmetric form. By laterally curving the facet edges, substantial reductions in rms error were effected, most notably in nonshallow reflectors, for facets with square projections onto the plane tangent to the vertex. However, a constraint imposed on the analysis apparently led to the requirement that adjacent facet edges have curvatures of opposite sign. This led to the conclusion that curving the edges of the center facet in an axisymmetric reflector offered no improvement over the best-fit flat facet.

The present paper also explores the possibility of using membrane facets with optimal edge curvatures. It is assumed that the reflector is shallow; hence, it can be modeled by an assemblage of nominally identical triangles or rectangles, and single-facet error calculations can be taken as representative of the entire reflector. Also, it is assumed that the reflecting material experiences approximately isotropic tensile loading. Linear membrane theory is used to analyze facet deformations.

Exact solutions are found for the lateral deflection of membranes in the shape of equilateral triangles and rectangles with prescribed parabolic edge deflections. These solutions are used to obtain expressions for the mean-square error between the ideal surface and the membrane facet. Minimization of the mean-square error yields optimum values of the radius of curvature of the deflected membrane edges and the center offset between the membrane and the ideal surface. These optimum values are used to calculate the minimum rms error.

Presented as Paper 83-1021 at the AIAA/ASME/AHS/ASCE 24th Structures, Structural Dynamics and Materials Conference, Lake Tahoe, Nev., May 2-4, 1983; received July 5, 1983; revision received Nov. 28, 1983. Copyright © American Institute of Aeronautics and Astronautics, Inc., 1983. All rights reserved.

*Aerospace Engineer, Structures and Dynamics Division.

Analysis

Figure 1 contains a sketch of a representative shallow, flat-faceted reflector with vertex radius of curvature R_0. In the present study, a typical flat facet is assumed to be replaced by a membrane with parabolically deflected edges. The object of the analysis is to ascertain the optimum parabolic edge deflection of the membrane and its optimum location on the normal to the ideal surface, the optimum values being those which together minimize the rms error between the membrane facet and a corresponding facet of the ideal surface.

Procedure

With the origin of rectangular Cartesian coordinates at the vertex, the ideal paraboloidal surface with radius of curvature R_0 at its vertex has the equation

$$z(x,y) = (x^2+y^2)/2R_0 \tag{1}$$

The small deflections $w(x,y)$ of a membrane under isotropic tension are, in the absence of lateral pressure, governed by the equation

$$\frac{\partial^2 w}{\partial x^2} + \frac{\partial^2 w}{\partial y^2} = 0 \tag{2}$$

The solution to Eq. (2) satisfying appropriate conditions on the boundary of the triangular or rectangular membrane facets is used along with Eq. (1) to define the mean-square error between the membrane facet and the ideal surface facet, i.e.,

$$\delta^2_{\text{rms}} = \frac{1}{A}\int_S\int (w-z)^2 \mathrm{d}A \tag{3}$$

In Eq. (3) the integration is over the appropriate planar triangular or rectangular region S having area A. The mean-square error is then minimized with respect to R, the radius of curvature of the assumed parabolic edge deflection (in the

case of the rectangle, R_1 and R_2) and h, an adjustment to the center offset between the membrane and the ideal surface. This process yields algebraic equations in R and h (R_1, R_2, and h for the rectangle) which, in turn, are used to calculate the minimum rms error.

Equilateral Triangles

Consider an equilateral triangular membrane facet with edges of length L and center at the origin of coordinates (x,y,z) (Fig. 2). The deflection that satisfies Eq. (2) and has parabolic form with radius of curvature R on all edges is

$$w(x,y) = -(\sqrt{3}/3RL)x(x^2-3y^2)$$

This solution is a modification of the St. Venant solution for torsion of a bar of equilateral triangular cross section.[3] Translating the membrane in the z direction by the dimensionless amount h,

$$w(x,y) = \frac{L^2}{2R}\left\{h - \frac{2\sqrt{3}}{3}\frac{x}{L}\left(\frac{x^2-3y^2}{L^2}\right)\right\} \tag{4}$$

To minimize the mean-square error, we require

$$\frac{\partial}{\partial R}\delta^2_{\text{rms}} = \frac{\partial}{\partial h}\delta^2_{\text{rms}} = 0$$

which yields

$$\iint_S (w-z)\frac{\partial w}{\partial R}\,dA = \iint_S (w-z)\frac{\partial w}{\partial h}\,dA = 0$$

or, finally,

$$\iint_S \left\{h - \frac{2\sqrt{3}}{3}\frac{x}{L}\left(\frac{x^2-3y^2}{L^2}\right)\right\}^2 dA - \frac{R}{R_0}\iint_S \left\{h - \frac{2\sqrt{3}}{3}\frac{x}{L}\left(\frac{x^2-3y^2}{L^2}\right)\right\}\left(\frac{x^2+y^2}{L^2}\right)dA = 0 \tag{5}$$

and

$$\iint_S \left\{h - \frac{2\sqrt{3}}{3}\frac{x}{L}\left(\frac{x^2-3y^2}{L^2}\right)\right\}dA - \frac{R}{R_0}\iint_S \frac{x^2+y^2}{L^2}\,dA = 0 \tag{6}$$

With the change of variables $(x/L,\ y/L) = (r/\sqrt{3},\ s/3)$, and the definitions

$$I_1 = \int_{-1}^{1/2}\int_0^{r+1} ds\,dr, \quad I_2 = \frac{2}{9}\int_{-1}^{1/2}\int_0^{r+1} r(r^2-s^2)\,ds\,dr$$

$$I_3 = \frac{4}{81}\int_{-1}^{1/2}\int_0^{r+1} r^2(r^4-2r^2s^2+s^4)\,ds\,dr$$

$$I_4 = \int_{-1}^{1/2}\int_0^{r+1} (r^2+\tfrac{1}{3}s^2)\,ds\,dr$$

$$I_5 = \int_{-1}^{1/2}\int_0^{r+1} r(r^4-\tfrac{2}{3}r^2s^2+s^4)\,ds\,dr$$

Eqs. (5) and (6) become

$$I_1h^2 - 2I_2h + I_3 = (R/3R_0)(I_4h - I_5) \tag{7}$$

and

$$I_1h - I_2 = (R/3R_0)I_4 \tag{8}$$

For the optimum values of R and h, Eqs. (7) and (8) yield

$$R = 3R_0\frac{I_1I_3 - I_2^2}{I_2I_4 - I_1I_5}, \quad h = \frac{I_3I_4 - I_2I_5}{I_2I_4 - I_1I_5}$$

The exact values are found to be

$$R = (7/10)R_0, \quad h = 13/360 \tag{9}$$

Hence, the membrane which yields the minimum mean-square error has equation

$$w(x,y) = \frac{5L^2}{7R_0}\left\{\frac{13}{360} - \frac{2\sqrt{3}}{3}\frac{x}{L}\left(\frac{x^2-3y^2}{L^2}\right)\right\} \tag{10}$$

Substituting Eqs. (1) and (10) into Eq. (3) and performing the integration gives, for the mean-square error, exactly

$$\delta^2_{\text{rms}} = \frac{3}{62{,}720}\frac{L^4}{F^2}$$

where $F = \frac{1}{2}R_0$ is the focal length of the ideal surface. Hence,

$$\frac{\delta_{\text{rms}}}{D} = \frac{\sqrt{15}}{560}\frac{(L/D)^2}{F/D} \tag{11}$$

where D is the diameter of a shallow circular reflector dish.

For comparison, values of δ_{rms}/D for two additional configurations are presented. The best-fit flat-facet configuration is obtained by assuming $w(x,y) = \text{const}$, and determining the constant for which δ^2_{rms} is a minimum. The resulting error is

$$\frac{\delta_{\text{rms}}}{D} = \frac{\sqrt{15}}{240}\frac{(L/D)^2}{F/D} \tag{12}$$

in agreement with Ref. 1.

The congruent-edge membrane configuration is obtained by giving the membrane edges the same curvature as the ideal surface, i.e., $R = R_0$, and minimizing δ^2_{rms} with respect to h only.

The result is

$$\frac{\delta_{\text{rms}}}{D} = \frac{\sqrt{21}}{560}\frac{(L/D)^2}{F/D} \tag{13}$$

Single-facet illustrations of the membrane configurations analyzed are shown in Fig. 3, where, for illustrative purposes, the deflection shapes are inverted and greatly exaggerated. Also, a contour plot for the optimum membrane facet is presented in Fig. 4. In addition to the nine equally spaced level curves in Fig. 4, the membrane's intersections with the ideal surface are also shown.

Rectangles

Consider a rectangular membrane facet of length $2a$, width $2b = 2\lambda a$, with $0 < \lambda \le 1$, and center at the origin (Fig. 5). Whereas the solution to the equilateral triangular membrane problem is algebraic, the rectangular membrane problem requires a Fourier series solution. The specification of parabolic deflections on the four boundaries takes the form

$$w(x, \pm\lambda a) = \frac{a^2}{2R_1}\left(\frac{x^2}{a^2} - 1\right)$$

and

$$w(\pm a, y) = \frac{\lambda^2 a^2}{2R_2}\left(\frac{y^2}{\lambda^2 a^2} - 1\right) \tag{14}$$

The deflection shape satisfying the Laplace equation and Eqs. (14), with the addition of a nondimensional normal translation h, is

$$w(x,y)=\frac{a^2}{2R_0}\left\{\frac{R_0}{R_1}w_1(x,y)+\lambda^2\frac{R_0}{R_2}w_2(x,y)+h\right\} \tag{15}$$

where

$$w_1(x,y)=\frac{32}{\pi^3}\sum_{n\ \text{odd}}^{\infty}\frac{(-1)^{(n+1)/2}}{n^3\cosh(n\pi\lambda/2)}\cos\frac{n\pi x}{2a}\cosh\frac{n\pi y}{2a} \tag{16}$$

and

$$w_2(x,y)=\frac{32}{\pi^3}\sum_{n\ \text{odd}}^{\infty}\frac{(-1)^{(n+1)/2}}{n^3\cosh(n\pi/2\lambda)}\cosh\frac{n\pi x}{2\lambda a}\cos\frac{n\pi y}{2\lambda a} \tag{17}$$

The ideal surface is again described by Eq. (1).

In this case, the object is to minimize the mean-square error with respect to R_1, R_2, and h. Hence, with the mean-square error again defined by Eq. (3), we require

$$\frac{\partial}{\partial h}\delta_{\text{rms}}^2=\frac{\partial}{\partial R_1}\delta_{\text{rms}}^2=\frac{\partial}{\partial R_2}\delta_{\text{rms}}^2=0 \tag{18}$$

which leads to the following equations determining the optimum values of R_1, R_2, and h:

$$h=L_1-\frac{R_0}{R_1}L_2-\lambda^2\frac{R_0}{R_2}L_3 \tag{19}$$

$$L_2h=L_4-\frac{R_0}{R_1}L_5-\lambda^2\frac{R_0}{R_2}L_6 \tag{20}$$

$$L_3h=L_7-\frac{R_0}{R_1}L_6-\lambda^2\frac{R_0}{R_2}L_8 \tag{21}$$

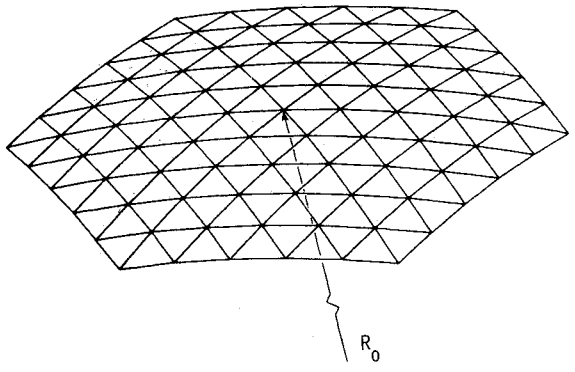

Fig. 1 Typical shallow flat-faceted reflector.

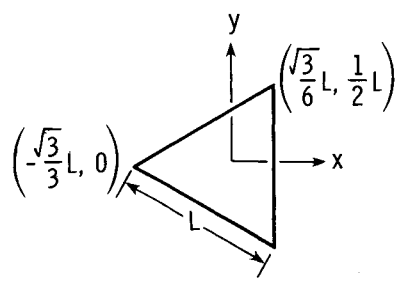

Fig. 2 Equilateral triangle in rectangular coordinate system.

With dimensionless quantities defined by

$$\bar{x}=\frac{x}{a},\quad \bar{y}=\frac{y}{\lambda a},\quad \bar{z}=\frac{2R_0}{a^2}z,\quad \bar{w}_1=\frac{2R_0}{a^2}w_1,\quad \bar{w}_2=\frac{2R_0}{a^2}w_2 \tag{22}$$

the coefficients $L_1,\ldots,L_8$ are given by

$$L_1(\lambda)=\int_0^1\int_0^1\bar{z}\,d\bar{y}\,d\bar{x}=\tfrac{1}{3}(1+\lambda^2) \tag{23}$$

$$L_2(\lambda)=\int_0^1\int_0^1\bar{w}_1\,d\bar{y}\,d\bar{x}=-\frac{128}{\pi^5\lambda}\sum_{n\ \text{odd}}^{\infty}\frac{\tanh(n\pi\lambda/2)}{n^5} \tag{24}$$

$$L_3(\lambda)=\int_0^1\int_0^1\bar{w}_2\,d\bar{y}\,d\bar{x}=L_2\left(\frac{1}{\lambda}\right) \tag{25}$$

$$L_4=\int_0^1\int_0^1\bar{z}\bar{w}_1\,d\bar{y}\,d\bar{x}=\frac{8}{15} \tag{26}$$

$$L_5(\lambda)=\int_0^1\int_0^1\bar{w}_1^2\,d\bar{y}\,d\bar{x}$$

$$=\frac{512}{\pi^7\lambda}\sum_{n\ \text{odd}}^{\infty}\frac{1}{n^7}\left(\frac{1+2n\pi e^{-n\pi\lambda}-e^{-2n\pi\lambda}}{1+2e^{-n\pi\lambda}+e^{-2n\pi\lambda}}\right) \tag{27}$$

$$L_6(\lambda)=\int_0^1\int_0^1\bar{w}_1\bar{w}_2\,d\bar{y}\,d\bar{x}$$

$$=\frac{4096}{\pi^8}\sum_{n\ \text{odd}}^{\infty}\sum_{m\ \text{odd}}^{\infty}\frac{1}{m^2n^2(m^2+\lambda^2n^2)^2} \tag{28}$$

$$L_7(\lambda)=\int_0^1\int_0^1\bar{z}\bar{w}_2\,d\bar{y}\,d\bar{x}=\lambda^2L_4 \tag{29}$$

$$L_8(\lambda)=\int_0^1\int_0^1\bar{w}_2^2\,d\bar{y}\,d\bar{x}=L_5\left(\frac{1}{\lambda}\right) \tag{30}$$

Since all the series in Eqs. (24-30) converge rapidly, only a few terms are needed for their accurate evaluation for every λ of interest.

After the optimum values of R_1, R_2, and h are obtained for a specified value of λ, they are then inserted into the mean-

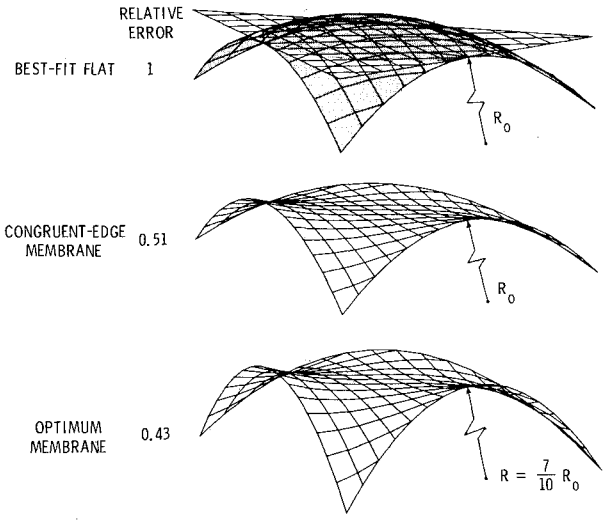

Fig. 3 Triangular ideal surface facet and membrane facets.

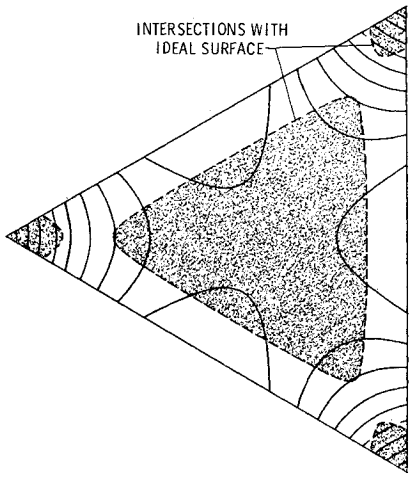

Fig. 4 Contour plot of deflection shape of optimum membrane facet.

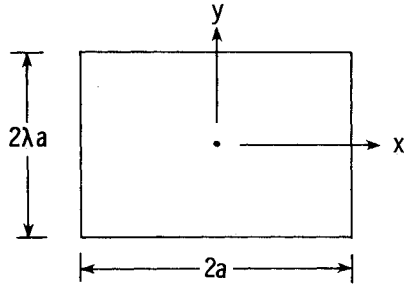

Fig. 5 Rectangle of sides $2a$ and $2\lambda a$ in rectangular coordinate system.

square error expression

$$\delta^2_{\text{rms}} = \left(\frac{a^2}{2R_0}\right)^2 \left\{ L_9 - 2hL_1 + h^2 + \left(\frac{R_0}{R_1}\right)^2 L_5 + \lambda^4 \left(\frac{R_0}{R_2}\right)^2 L_8 + 2\lambda^2 \frac{R_0^2}{R_1 R_2} L_6 + 2\frac{R_0}{R_1}(L_4 - hL_2) + 2\lambda^2 (L_7 - hL_3) \right\} \tag{31}$$

where

$$L_9(\lambda) = \int_0^1 \int_0^1 \bar{z}^2 \, d\bar{y} \, d\bar{x} = \frac{8}{15}\left(1 + \frac{5}{3}\lambda^2 + \lambda^4\right) \tag{32}$$

Similar calculations have also been performed for some related configurations. The best-fit flat-facet configuration is obtained by normal translation of the $w(x,y) = \text{const}$ facet to its minimum δ_{rms} position. The congruent-edge membrane configuration is obtained by giving the edges of the membrane the same curvature as the ideal surface, i.e., $R_1 = R_2 = R_0$, and minimizing δ^2_{rms} with respect to h only. Still another configuration is obtained by specifying equal curvatures on all edges, i.e., $R_1 = R_2 = R$, and minimizing δ^2_{rms} with respect to R and h. In Fig. 6, single-square-facet illustrations are shown for all but the last membrane configuration, which yielded results quite similar to those of the more general $R_1 \neq R_2$ case. (In fact, for square facets, the results are identical.) Again, the geometric features are exaggerated for illustrative purposes.

Results and Discussion

Equilateral Triangles

The rms errors are given in Table 1 for the flat-facet and membrane-facet configurations illustrated in Fig. 3. The rms

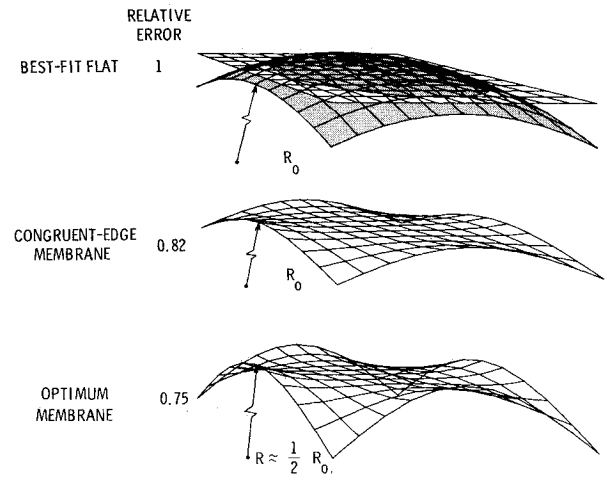

Fig. 6 Square ideal surface facet and membrane facets.

Table 1 rms errors for equilateral triangular facets

Facet configuration	$\frac{F/D}{(L/D)^2}\frac{\delta_{\text{rms}}}{D}$	Relative error
Best-fit flat	$\sqrt{15}/240 = 0.0161$	1.00
Congruent-edge membrane	$\sqrt{21}/560 = 0.0082$	0.51
Optimum membrane	$\sqrt{15}/560 = 0.0069$	0.43

error for the congruent-edge ($R = R_0$) configuration is about 49% below the error for the best-fit flat-facet configuration. Such an improvement in surface accuracy might justify the additional fabrication effort that would likely be required to produce a congruent-edge membrane configuration. The optimum membrane-facet configuration yields only a modest additional improvement in accuracy. Also, because of its greater edge curvature, the optimum membrane-facet configuration ($R = 7/10\ R_0$) would give a faceted reflector surface a more pronounced scalloped effect, which might adversely affect reflector performance. Hence, in light of its marginal additional gains in accuracy, the use of the optimum membrane configuration in a faceted reflector may be difficult to justify.

Rectangles

The rms errors are given in Table 2 for the flat-facet and three membrane-facet configurations, two of which are illustrated for squares in Fig. 6. The flat-facet case is again amenable to closed-form evaluation. The result is

$$\frac{\delta_{\text{rms}}}{D} = \frac{\sqrt{5}}{120}\sqrt{1+\lambda^4}\,\frac{(2a/D)^2}{F/D}$$

which, for a square, is in agreement with Ref. 1.

Again, the best-fit flat-facet configuration is least accurate. However, the membrane facets offer considerably less improvement over the flat-facet results than was the case with equilateral triangles, the maximum rms error reduction being about 25% for square facets compared with about 55% for the triangles. The large reductions in rms error for the elongated rectangles are somewhat misleading, since a flat-faceted reflector design would not be likely to contain high aspect ratio (small λ) facets. A more realistic appraisal of the error reductions for the high aspect ratio facets can be gained by viewing them as the result of the addition of properly curved internal supports to an initially square facet. Clearly,

Table 2 Normalized rms error for rectangular facets

Facet configuration	$\frac{F/D^{a}}{(2a/D)^2}\frac{\delta_{rms}}{D}$ $\lambda = 1.0$	0.8	0.6	0.4	0.2
Best-fit flat	1(0.0264)	0.84	0.75	0.72	0.71
Congruent-edge membrane	0.83	0.64	0.43	0.22	0.06
Optimum membrane[b]	0.75	0.60	0.39	0.19	0.05
Optimum membrane[c]	0.75	0.58	0.38	0.19	0.05

[a] $F = \frac{1}{2}R_I$. [b] Same curvature on all edges ($R_1 = R_2$). [c] Same curvature on opposite edges ($R_1 \neq R_2$).

Table 3 Normalized rms error for equal-area facets

Facet configuration	$\frac{F/D}{(L/D)^2}\frac{\delta_{rms}}{D}$ Rectangle,[c] $\lambda =$ 1.0	0.8	0.6	0.4	0.2	Equilateral triangle
Best-fit flat	1(0.0114)	1.05	1.25	1.79	3.54	1.41
Congruent-edge membrane	0.83	0.80	0.72	0.54	0.28	0.72
Optimum membrane[a]	0.75	0.75	0.64	0.48	0.26	0.61
Optimum membrane[b]	0.75	0.73	0.63	0.47	0.26	—

[a] Same curvature on all edges. [b] Same curvature on opposite edges. [c] For equal facet area, $a^2 = \sqrt{3}L^2/16\lambda$.

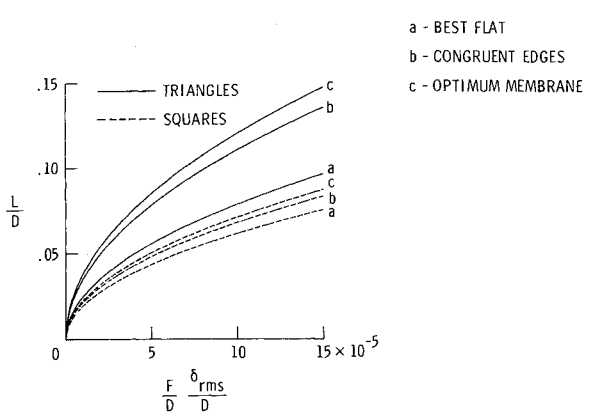

Fig. 7 Maximum member length meeting rms error criterion for faceted reflector surface.

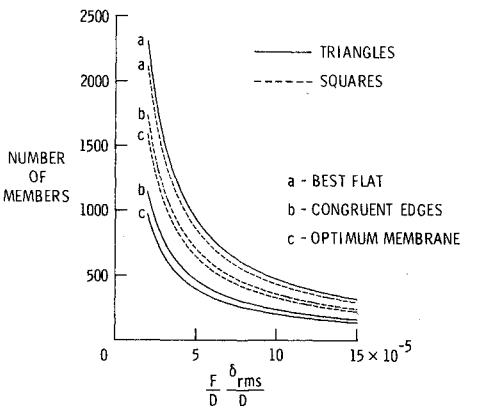

Fig. 8 Number of members required to meet rms error criterion for faceted reflector surface.

such additional supporting structure would greatly reduce the rms error, but at significant costs in fabrication, complexity, and structural weight.

It might also be noted here that if $2a$ is replaced by L in Table 2, then Tables 1 and 2 can be used together to determine the maximum triangular or rectangular facet edge (or structural member) length L that will satisfy a prescribed rms error criterion. An illustration for a shallow circular reflector composed of nominally identical equilateral triangles or squares is provided by Fig. 7, where the maximum dimensionless member length required to satisfy a given error criterion, L/D, is plotted as a function of the dimensionless rms error, $F/D\,\delta_{rms}/D$.

The results can also be used to approximate the number of equal-length structural members required to satisfy a given error criterion. With the number of required facets given approximately by

$$N_f = (\pi/\sqrt{3})(D/L)^2 \text{ for triangles}$$

$$= (\pi/4)(D/L)^2 \text{ for squares}$$

and the number of members being approximately

$$N_m = (3/2)N_f + \sqrt{3/2N_f} \text{ for triangles}$$

$$= 2(N_f + \sqrt{N_f}) \text{ for squares}$$

the results for triangles and squares from Tables 1 and 2 yield the estimates shown in Fig. 8.

Equal-Area Facets

A comparison of results for triangles and rectangles of equal area, which will be of interest if facet area rather than facet edge length is a controlling parameter, is facilitated by Table 3. The results suggest the following conclusions for flat facets:

1) Equilateral triangles are more accurate than squares with the same edge length.

2) Equilateral triangles are less accurate than squares with the same area.

3) The most accurate rectangular facet is the square.

For curved-edge membrane facets, the results indicate that:

1) Membrane facets are more accurate than flat facets.

2) Equilateral triangles are more accurate than squares with the same edge length or the same area.

3) For comparable rms error, triangles allow the use of longer and/or fewer members than squares.

4) Optimum configurations produce "scalloped" surfaces while offering little improvement in accuracy over the congruent-edge configurations.

Concluding Remarks

It has been shown that the equilateral triangular or rectangular segment of a shallow paraboloidal (or spherical) surface can be replaced with considerably less rms error by an appropriately deformed membrane facet rather than a flat facet. This result suggests that a reflecting mesh, stretched with approximately isotropic tension over a framework of appropriately curved members, could produce a more accurate antenna than the similar flat-faceted reflector, or an equally accurate reflector with larger facets and, hence, fewer structural members. The results are based on the linear theory of membranes under isotropic tension, and assume that the reflector is shallow enough to have essentially equal principal curvatures. Possibly fruitful extensions of this work might include investigations of the effects of nonuniform mesh tension or stiffness, or nonlinear membrane theory. A reflector design based on the present results would also have a scalloped surface, the effects of which on antenna performance might also warrant examination.

Acknowledgment

Valuable contributions to this work by Catherine L. Herstrom, NASA Langley Research Center, who performed numerous calculations and generated most of the figures, are gratefully acknowledged.

References

[1] Agrawal, P. K., Anderson, M. S., and Card, M. F., *IEEE Transactions on Antennas and Propagation*, Vol. AP-29, July 1981, pp. 688-694.

[2] Meyer, R. X., "Precision of Mesh-Type Reflectors for Large Space-Borne Antennas," AIAA Paper 82-0652, May 1982.

[3] Timoshenko, S., and Goodier, J. N., *Theory of Elasticity*, 2nd Ed., McGraw-Hill Book Co., New York, 1951, p. 266.

From the AIAA Progress in Astronautics and Aeronautics Series

AERODYNAMICS OF BASE COMBUSTION—v. 40

Edited by S.N.B. Murthy and J.R. Osborn, Purdue University, A. W. Barrows and J. R. Ward, Ballistics Research Laboratories

It is generally the objective of the designer of a moving vehicle to reduce the base drag—that is, to raise the base pressure to a value as close as possible to the freestream pressure. The most direct and obvious method of achieving this is to shape the body appropriately—for example, through boattailing or by introducing attachments. However, it is not feasible in all cases to make such geometrical changes, and then one may consider the possibility of injecting a fluid into the base region to raise the base pressure. This book is especially devoted to a study of the various aspects of base flow control through injection and combustion in the base region.

The determination of an optimal scheme of injection and combustion for reducing base drag requires an examination of the total flowfield, including the effects of Reynolds number and Mach number, and requires also a knowledge of the burning characteristics of the fuels that may be used for this purpose. The location of injection is also an important parameter, especially when there is combustion. There is engineering interest both in injection through the base and injection upstream of the base corner. Combustion upstream of the base corner is commonly referred to as external combustion. This book deals with both base and external combustion under small and large injection conditions.

The problem of base pressure control through the use of a properly placed combustion source requires background knowledge of both the fluid mechanics of wakes and base flows and the combustion characteristics of high-energy fuels such as powdered metals. The first paper in this volume is an extensive review of the fluid-mechanical literature on wakes and base flows, which may serve as a guide to the reader in his study of this aspect of the base pressure control problem.

522 pp., 6×9, illus. $19.00 Mem. $35.00 List

TO ORDER WRITE: Publications Dept., AIAA, 1633 Broadway, New York, N.Y. 10019